Solid State Communications 202 (2015) 24–27

Contents lists available at ScienceDirect

Solid State Communications

journal homepage: www.elsevier.com/locate/ssc

Ferroelectric and ferromagnetic properties of $SrTi_{0.9}Fe_{0.1}O_{3-\delta}$ thin films

Y.G. Wang, X.G. Tang*, Q.X. Liu, Y.P. Jiang, Z.Y. Feng

School of Physics & Optoelectric Engineering, Guangdong University of Technology, Guangzhou Higher Education Mega Centre, Guangzhou 510006, PR China

ARTICLE INFO

Article history:
Received 22 March 2014
Received in revised form
19 October 2014
Accepted 1 November 2014
Communicated by T. Kimura
Available online 10 November 2014

Keywords:
A. $SrTiO_3$ films
B. Spin coating
D. Ferroelectric properties
D. Ferromagnetism

ABSTRACT

The $SrTi_{0.9}Fe_{0.1}O_{3-\delta}$ thin film grown on the $LaNiO_3$ coated Si(100) substrates was prepared by a sol–gel process. The structure, micrograph, chemical states, electrical and magnetic properties of the thin film were investigated by using X-ray diffractometor (XRD), atomic force microscopy (AFM), X-ray photoelectron spectroscopy (XPS), ferroelectric test system and vibrating sample magnetometer (VSM), respectively. The results showed that the ferroelectric properties with the saturated polarization ($2P_s$), remanent polarization ($2P_r$) and coercive field ($2E_c$) of 12.3 μC/cm^2, 1.58 μC/cm^2 and 33 kV/cm, respectively, at applied field of 200 kV/cm. The average remnant magnetization (M_r) and saturated magnetization (M_s) of the thin film were 3.74×10^{-2} and 9.22×10^{-2} emu/cm^3, respectively. Both the ferroelectric and ferromagnetic properties could be explained by the defect induced and the Fe ion substitution. Such multiferroic thin film was appropriate to be used in the field of multiferroic devices.

1. Introduction

Multiferroic materials, with the coexistence of at least two ferroic properties, have been of great interest due to their potential applications in memory devices, sensors and actuators [1]. However, since the competing electron configurations are required for ferroelectricity and ferromagnetism, these materials are rare in nature [2]. Strontium titanate $SrTiO_3$ is known as an incipient ferroelectric with high dielectric, low dielectric losses and high tenability, and has been widely applied in the electronically tunable microwave devices [3,4]. The bulk $SrTiO_3$ shows no ferroelectric or ferromagnetic properties; however, there are many ways that can be used to induce the ferroic properties in $SrTiO_3$. For example, the ferroelectric properties can be obtained by introducing the strain [5], substituting the O^{16} with O^{18} [6], or doping with other elements [7], and the ferromagnetic properties can be caused by ion irradiating [8], vacuum annealing [9] or transition-metal doping [10]. Among these, the Fe-doped $SrTiO_3$ has been proven to be a ferromagnetic with resistive switching characteristics [11], and can also be used in ozone gas sensor [12]. After substituting the Ti^{4+} with the Fe ions, the crystal symmetry of the $SrTiO_3$ can be decreased to a certain degree due to the different ionic radii of the Fe and Ti ions. Besides, Fe ions usually exhibit a mixed valence states of Fe^{2+}, Fe^{3+} and Fe^{4+} in the system [13], and oxygen vacancies is unavoidable in order to maintain the charge balance [10,14]. In addition to the generally observed strain in thin films, all these characteristics could promote the ferroelectric properties in the $SrTi_{1-x}Fe_xO_{3-\delta}$ system. However, because of the paraelectric nature of pure $SrTiO_3$, the possible ferroelectric applications of $SrTi_{1-x}Fe_xO_{3-\delta}$ have often been ignored. Till now, we can find only few researches about the ferroelectric properties of the $SrTi_{1-x}Fe_xO_{3-\delta}$ films [15], and the multiferroic behavior of the sol–gel derived $SrTi_{1-x}Fe_xO_{3-\delta}$ thin films has not been reported before.

In this work, $SrTi_{0.9}Fe_{0.1}O_{3-\delta}$ thin film grown on the $LaNiO_3$ coated Si(100) substrates was prepared by a sol–gel process. The ferroelectric and magnetic properties of the $SrTi_{0.9}Fe_{0.1}O_{3-\delta}$ thin film were investigated.

2. Experimental details

$SrTi_{0.9}Fe_{0.1}O_{3-\delta}$ (abbreviated as STF10) thin film was synthesized on the $LaNiO_3$ (LNO) coated Si(100) substrate by a sol–gel route with spin-coating process. To obtain the precursor solution, reagent-grade strontium acetate, iron nitrate nonahydrate and titanium butyrate were dissolved under continuous stirring at 60 °C in acetic acid, 2-methoxyethanol and acetyl acetone, respectively. The three solutions was then mixed and stirred at 60 °C for 1.5 h, forming a complete homogeneous transparent precursor solution. The concentration of the final solution was adjusted to 0.25 M with a pH value of 2–3. The LNO thin layer prepared by

* Corresponding author. Fax: +86 20 3932 2265.
E-mail address: xgtang@gdut.edu.cn (X.G. Tang).

http://dx.doi.org/10.1016/j.ssc.2014.11.001
0038-1098/

chemical solutions deposition was described in previous literatures [16]. The STF10 layers were spin-coated onto the LNO films in the same way and finally annealed at 650 °C for 15 min by rapid thermal annealing (RTA) furnace in air. The thickness of the as-grown thin films on Si(100) substrates was measured by a surface profiler (KLA-Tencor P-10, USA). The thicknesses of the LNO and STF10 thin films were about 80 nm and 100 nm, respectively.

The structure and micrograph of the STF10 thin film was identified by the X-ray diffractometer (XRD, Pgeneral XD-2, China) and atomic force microscopy (AFM, BenYuan CSPM-5500, China), respectively. The surface chemical states of the thin film were characterized by X-ray photoelectron spectroscopy (XPS, Thermo Fisher Scientific ESCALAB 250, USA) with Al Kα radiation source. For the electrical measurements, top gold (Au) electrodes of 0.2 mm diameter were deposited through a shadow mask onto the STF10 thin films by a vacuum evaporation. The ferroelectric properties (*P*–*E*) and the leakage current characteristics (*I*–*V*) were measured by a ferroelectric test system (Radiant Precision Premier II, USA). The room temperature magnetic properties of the film were measured by a vibrating sample magnetometer (VSM, Quantum Design PPMS-9, USA).

3. Results and discussion

The XRD patterns of the STF10 thin film grown on the LNO buffered Si(100) substrate was shown in Fig. 1(a). Three peaks, (100), (110) and (200) were observed in the XRD pattern of the STF10 thin films on LNO buffered Si(100) substrate which suggests a polycrystalline perovskite structure with a slight (110) preferred orientation [16]. The magnified plot of the peaks was presented in the inset of Fig. 1, which indicates the superposed peak of the LNO (110) and STF10 (110) clearly. The highly orientation of the LNO is related to concentration of precursor concentration [17], and the slight orientation of the STF10 thin can be ascribed to its quite similar lattice constant and crystal structure to LNO thin films. The image of the STF10 thin film was displayed in the Fig. 1(b), which exhibits a dense micro-structure with no cracks. The calculated results of the AFM image showed that the surface grain size is about 86 nm and the root mean square roughness of the STF10 thin film is 5.8 nm.

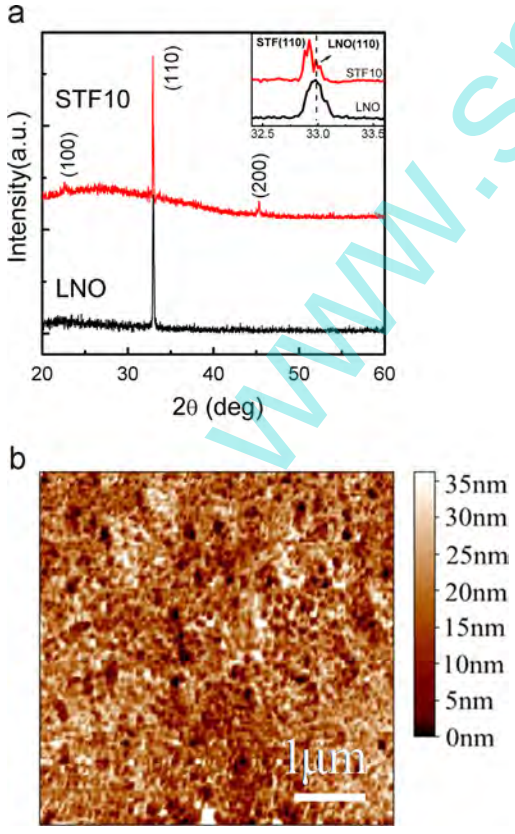

Fig. 1. (Color online) (a) XRD patterns of STF10 and LNO thin films, and (b) AFM image of the STF10 thin film. Inset shows the magnified plot of the peaks (110).

The composition of STF10 thin film was analyzed by XPS as well. The atomic ratio of Sr:Ti:Fe is found to be 10.35:10.49:2.35, which slightly deviated from the theoretical value of 10:9:1 of stoichiometric thin film. Besides the analytical error, the deviation may be relevant with the presence of divalent Fe ions. Since the ions can be incorporated in the SrO sublattice, higher Fe concentration may indicate its migration towards extended defects and surface [18], which is however not sufficient to kill the long range atomic order. The valence states of the Fe ions in STF10 thin film characterized by XPS were shown in Fig. 2. The Fe 2p 2/3 and 2p 1/2 doublets of STF10 were seen in the vicinity of 706 eV (705.5, 707.3 eV) and 721.76 eV, respectively. These peaks appear at lower binding energy compared to measurements on Fe_2O_3 with Fe^{3+} [10], implying the existence of Fe^{2+} and Fe^{3+} in STF10. The clear Fe^{3+} satellite peak was present at 718.48 eV. The peak at 711.6 eV is about 0.9 eV higher than the Fe 2p 2/3 of Fe_2O_3, indicating the possible existence of Fe^{4+}. Thus, the XPS result shows the coexistence of Fe^{2+}, Fe^{3+} and Fe^{4+} mixed valence states in STF10 thin film, with dominance of the Fe^{3+} states, which is consistent with the previous works and corresponds to the existence of oxygen vacancies [10].

Fig. 3 displays the polarization–electric filed (*P*–*E*) hysteresis loop of the STF10 thin film. The loop showed an almost perfect symmetry along both the electric field axes and the polarization axes, indicating the existence of ferroelectric properties. The obtained values of double saturated polarization ($2P_s$), remanent polarization ($2P_r$) and coercive field ($2E_c$) at the applied *E* of 200 kV/cm were 12.3 μC/cm^2, 1.58 μC/cm^2 and 33 kV/cm, respectively. The improved ferroelectric properties in STO could be explained by the defect induced by the Fe ion substitution [15]. Based on the XPS results, Fe ions exhibit a mixed valence of +4/+3/+2. When substitute the Ti^{4+} with the Fe ion in the STO lattice, oxygen vacancies ($V_{\ddot{O}}$) are generally created in order to maintain the charge balance [10,19], forming the defect dipoles of cations (*i.e.* Fe ions)-$V_{\ddot{O}}$ complex, therefore increasing the total polarization [20]. Besides that, the internal strain and the decrease of crystal symmetry induced by the misfit of substrate and aliovalent ionic substitution may also be beneficial for the enhancement of spontaneous [21].

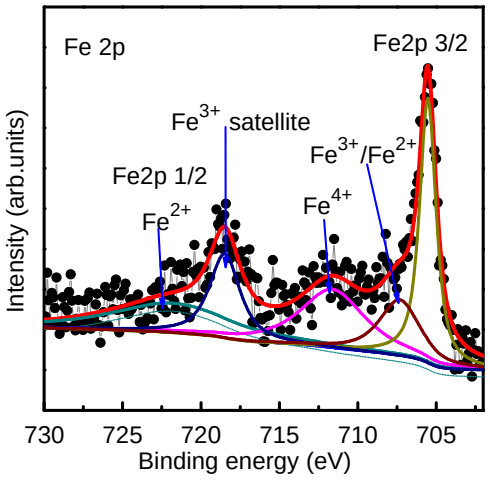

Fig. 2. (Color online) Fe 2p XPS splitting spectrum of the STF10 thin film on LNO/Si (100) substrate.

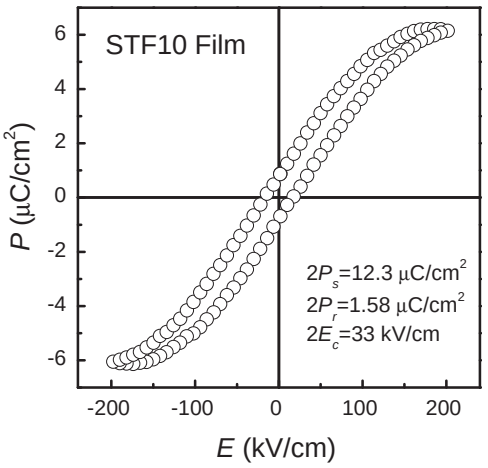

Fig. 3. *P–E* hysteresis loop of the STF10 thin film on LNO/Si(100) substrate.

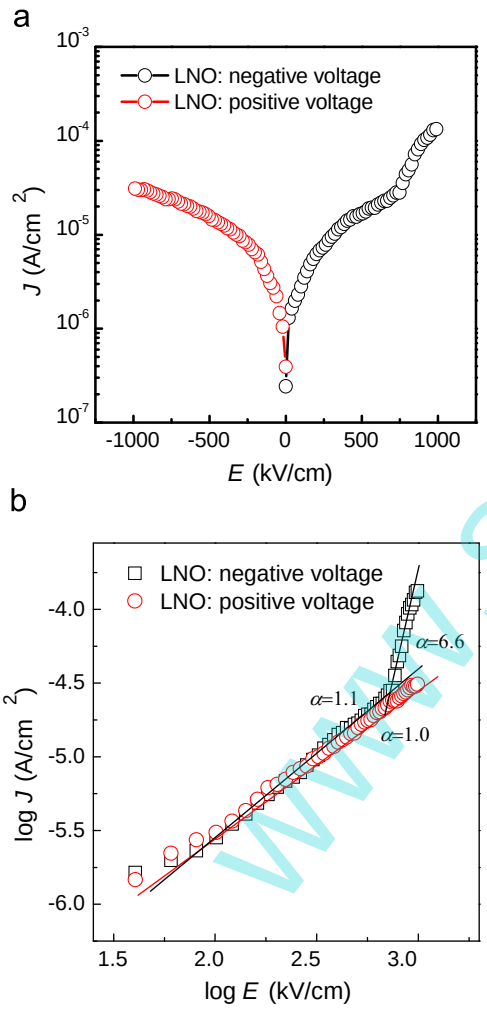

Fig. 4. (Color online) (a) Leakage current curves of the STF10 thin film on LNO/Si (100) substrate, and (b) log J versus log E plot of the STF10 thin film. The straight lines show the fitted linear segments of the plots.

Fig. 4(a) shows the leakage current densities (J) as a function of electric field (E) with the bottom LNO electrode having a dc bias voltage ranged from −9.9 to 9.9 V for the STF10 thin film. The leakage current densities of the STF10 thin films were about 2.76×10^{-6} and 1.6×10^{-5} A/cm^2, respectively, at applied field of 100 and 500 kV/cm, which is low enough to provide the potential application in dielectric devices. In order to analyze the leakage

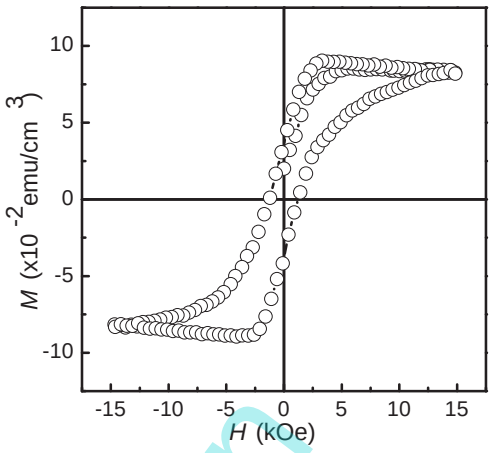

Fig. 5. *M–H* curve of the STF10 thin film on LNO/Si(100) substrate.

conduction mechanisms of the SFT10 films leakage curves are divided into several regions and the slopes ($\alpha=\log J/\log E$) of each region are fitted, as shown in Fig. 4(b). When a positive dc bias voltage was applied to the bottom LNO electrode, the α values of the BNF film is 1.0, which indicates the thermally simulated free electrons dominated Ohmic conduction behavior for BFT/LNO interface [22]. When a negative dc bias voltage was applied to the bottom LNO electrode, the α values of the BNF films are 1.1 and 6.6, respectively at low and high electric field. The leakage follow the Ohmic conduction at the electric field of <710 kV/cm, and follow the space–charge–limited current (SCLC) mechanisms at the electric field of >710 kV/cm [23,24].

The room temperature magnetization of the STF10 thin film as a function of in-plane external magnetic field in the range of −15 to 15 kOe was shown in Fig. 5. Hysteresis loop characteristic of weak ferromagnetism was clearly observed in the figure. The average remnant magnetization (M_r), saturated magnetization (M_s) and coercive magnetic field (H_c) are 3.74×10^{-2} emu/cm^3, 9.22×10^{-2} emu/cm^3 and 1.23 kOe, respectively. Magnetoelastic effects may be an important contributor to the ferromagnetic properties in STF10 thin films [13]. Besides, the F-center exchange (FCE) mechanism can also be used to explain the ferromagnetism [25]. When F-center was formed by a $V_{Ö}$-trapped electron, the electron will occupy an orbital which overlaps the d shells of both Fe^{3+} neighbors, thereby forming the ferromagnetic exchange interaction through the help of Fe^{3+}–$V_{Ö}$–Fe^{3+} complex.

4. Conclusions

In summary, the multiferroic $SrTi_{0.9}Fe_{0.1}O_{3-\delta}$ thin film was synthesized on the $LaNiO_3$ coated Si(100) substrates by the sol–gel process. The double saturated polarization ($2P_s$), average remnant magnetization (M_r) and saturated magnetization (M_s) of the STF10 thin film were 12.3 μC/cm^2, 3.74×10^{-2} emu/cm^3 and 9.22×10^{-2} emu/cm^3, respectively. Both the ferroelectric and magnetic properties could be explained by the defect induced by the Fe ion substitution. The leakage current density of the STF10 thin film was about 2.76×10^{-6} A/cm^2 at applied field of 100 kV/cm. Such thin film was appropriate to be used in the field of multiferroic devices.

Acknowledgments

This work was supported by the National Natural Science Foundation of China (Grant nos. 11032010 and 11202054), and

the Guangdong Provincial Educational Commission of China (Grant no. 2012KJCX0044).

References

[1] W. Eerenstein, N.D. Mathur, J.F. Scott, Nature 442 (2006) 759.
[2] K.C. Verma, J. Kaur, N.S. Negi, R.K. Kotnala, Solid State Commun. 178 (2014) 11.
[3] K.A. Müller, H. Burkard, Phys. Rev. B 19 (1979) 3593.
[4] R.C. Neville, B. Hoeneisen, C.A. Mead, J. Appl. Phys. 43 (1972) 2124.
[5] W.J. Maeng, I. Jung, J.Y. Son, Solid State Commun. 152 (2012) 1256.
[6] M. Itoh, R. Wang, Y. Inaguma, T. Yamaguchi, Y.-J. Shan, T. Nakamura, Phys. Rev. Lett. 82 (1999) 3540.
[7] D.A. Tenne, A. Soukiassian, X.X. Xi, H. Choosuwan, R. Guo, A.S. Bhalla, Phys. Rev. B 70 (2004) 174302.
[8] K. Potzger, J. Osten, A.A. Levin, A. Shalimov, G. Talut, H. Reuther, S. Arpaci, D. Bürger, H. Schmidt, T. Nestler, D.C. Meyer, J. Magn. Magn. Mater. 323 (2011) 1551.
[9] D.A. Crandles, B. DesRoches, F.S. Razavi, J. Appl. Phys. 108 (2010) 053908.
[10] D.H. Kim, N.M. Aimon, L. Bi, G.F. Dionne, C.A. Ross, J. Appl. Phys. 111 (2012) 07A918.
[11] T. Menke, P. Meuffels, R. Dittmann, K. Szot, R. Waser, J. Appl. Phys. 105 (2009) 066104.
[12] V.R. Mastelaro, S.C. Zílio, L.F. da Silva, P.I. Pelissari, M.I.B. Bernardi, J. Guerin, K. Aguir, Sens. Actuators B 181 (2013) 919.
[13] D.H. Kim, L. Bi, P. Jiang, G.F. Dionne, C.A. Ross, Phys. Rev. B 84 (2011) 014416.
[14] L.H. Brixner, Mater. Res. Bull. 3 (1968) 299.
[15] A.S. Kumar, P. Suresh, M.M. Kumar, H. Srikanth, M.L. Post, K. Sahner, R. Moos, S. Srinath, J. Phys. Conf. Ser. 200 (2010) 092010.
[16] X.G. Tang, H.L.W. Chan, A.L. Ding, Appl. Surf. Sci. 207 (2003) 63.
[17] H. Miyazaki, T. Goto, Y. Miwa, T. Ohno, H. Suzuki, T. Ota, M. Takahashi, J. Eur. Ceram. Soc. 24 (2004) 1005.
[18] J. Szade, K. Szot, M. Kulpa, J. Kubacki, C. Lenser, R. Dittmann, R. Waser, Phase Transit. 84 (2011) 489.
[19] I. Denk, W. Münch, J. Maier, J. Am. Ceram. Soc. 78 (1995) 3265.
[20] W.L. Warren, G.E. Pike, K. Vanheusden, D. Dimos, B.A. Tuttle, J. Robertson, J. Appl. Phys. 79 (1996) 9250.
[21] N.A. Hill, J. Phys. Chem. B 104 (2000) 6694.
[22] X.G. Tang, J. Wang, Y.W. Zhang, H.L.W. Chan, J. Appl. Phys. 94 (2003) 5163.
[23] P. Zubko, D.J. Jung, J.F. Scott, J. Appl. Phys. 100 (2006) 114113.
[24] X.G. Tang, J. Wang, X.X. Wang, H.L.W. Chan, Chem. Mater. 16 (2004) 5293.
[25] R.E. Venkata, S.M. Yang, R. Jung, M.H. Jung, B.W. Lee, C.U. Jung, J. Appl. Phys. 113 (2013) 187219.